RESEARCH COMMUNICATION

Correlation of CT Perfusion Images with VEGF Expression in Solitary Brain Metastases

Jian-Hua Zhang[1&], Ming-Sheng Wang[2&], Hai-Hong Pan[1], Shu-Feng Li[1], Zhong-Qiu Wang[1*], Wang-Sheng Chen[3*]

Abstract

Objectives: To obtain permeability surface (PS) values using multi-slice helical CT perfusion imaging and to evaluate the spatial distribution correlation between PS values and vascular endothelial growth factor (VEGF) expression in solitary brain metastases. Methods: Imaging was performed on 21 patients, PS values being calculated from the central, border and peripheral parts of tumours. VEGF expression was determined by immunohistochemical staining. Results: Rim enhancement was found in 16 cases, the border of the tumour featuring PS elevation with high VEGF expression in 13 cases. In the 5 cases with nodular enhancement, the border and the central part had high permeability and VEGF expression was high in all cases, the correlation being significant (P<0.01) . Conclusion: VEGF expression in brain metastases positively correlates with PS values from CT perfusion imaging, so that the latter can be used in the surveillance of angiogenic activity in brain metastases.

Keywords: Computed tomography - X-rays - PS value - vascular endothelial growth factor - metastases - brain

Asian Pacific J Cancer Prev, **13**, 1575-1578

Introduction

Brain metastases occur at any age, especially in those over the age of 40. The most common primary tumours are lung, breast and gastrointestinal tumours. In recent years, with the continuous emergence of cancer diagnosis and treatment, survival time has been prolonged, and with the extensive application of maturing imaging technology, more and smaller metastases are detected early. As a result, the clinical incidence of brain metastases continues to rise, accounting for about 40% of intracranial tumours (Petchell, 2003).

As a kind of tumour, the occurrence, development, invasion and metastasis of brain metastases are dependent on tumour angiogenesis. Folkman (1971) first proposed that tumour angiogenesis plays an important role in tumour biological behaviour. When the tumour grows to ~1-2 mm, it induces new blood vessel formation to supply nutrition. Studies have confirmed that tumour angiogenesis is not only a necessary condition for tumour growth, but also has an important role in the metastasis of malignant tumours (Hanahan & Folkman, 1996). Many treatment methods control cancers by directly or indirectly affecting tumour angiogenesis, tumour growth and metastasis (O'Reilly et al., 1997; Dhanabal et al., 1999; Dixelius et al., 2000). Vascular endothelial growth factor (VEGF), which can induce tumour angiogenesis and significantly increase vascular permeability, is the strongest regulatory factor. Therefore, VEGF has been a hot spot of research in recent years. There are many methods used to perform in vivo imaging of brain microvessels, such as PET, Xe-CT, MR and CT perfusion imaging (Miles et al., 1991; Wintermark et al., 2001; Principi et al., 2003). In early studies, CT perfusion imaging was used in the study of cerebral ischemia (Eastwood et al., 2001), and later also in brain tumour detection, location, classification and treatment monitoring (Cenic & Nabavi, 2000; Roberts et al., 2001; Roberts et al., 2002).

The treatment of brain metastases has become a great challenge to the medical profession today. Radiation techniques cut off the blood supply of the tumour to induce tumour tissue necrosis. The more abundant the blood supply, the more sensitive the tumour is to radiotherapy, leading to a more obvious therapeutic effect. Hermans et al. (2003) performed a CT perfusion study on 18 head and neck squamous cell carcinoma patients and found that tumours with poor perfusion are not sensitive to radiotherapy, while high perfusion tumours are radiation-sensitive. Clinically, it is generally accepted that the treatment effect of γ knife on blood-supplied brain metastases is best. CT perfusion studies of brain metastases have furthered our understanding of the molecular mechanisms of brain metastasis imaging. This study will provide a new treatment platform for treatment studies and make practical sense of observing radiation therapy effects (Hoeffner et al., 2004). There are currently

*[1]Department of Radiology, East Hospital, Tongji University School of Medicine, Shanghai, [2]Department of Neurosurgery, The First Affiliated Hospital of Xinxiang Medical University, Weihui, [3]Department of Radiology, Hainan Provincial Pepole's Hospital, Haikou, China [&]Equal contributors *For correspondence: zhq2001us@yahoo.com, zhutailin123@126.com, chenwangsheng463@sina.com*

no reports available on CT perfusion imaging being used to observe vascular permeability.

This report evaluated the correlation of CT perfusion imaging with VEGF expression through the analysis of multi-slice spiral CT perfusion imaging and histopathological examination of 21 cases of solitary brain metastases. We hope that this analysis with provide a reliable means of using imaging to monitor and evaluate the clinical treatment of brain metastases.

Materials and Methods

Clinical data

There were 21 cases of solitary brain metastases in our hospital, including 14 males and 7 females, from 2004 to 2005. These cases were all aged from 33 to 69 years, with a mean age of 51 years old. They were pathologically confirmed with metastatic carcinoma (15 cases were lung cancer, three cases were breast cancer, two cases were colon cancer and one case was renal carcinoma among the primary tumours). Sixteen patients underwent primary tumour resection, and the rest were confirmed to be the primary cancer by imaging or biopsy. All patients were preoperatively examined by multi-slice spiral CT perfusion imaging, and were not treated with any anti-brain tumour treatment. Lumps were round, supratentorial in 17 cases and infratentorial in four cases, and the average diameter was 2.8 cm. All of these cases were excised by surgery after 1 month of multi-slice spiral CT perfusion imaging.

Multi-slice spiral CT perfusion imaging method

A GE Lightspeed TM 16i MSCT machine was used. For the first conventional CT, a thickness of 10 mm was used to determine the tumour location, then the same multi-layer MSCT technology (toggling-table skill) was applied to the tumour perfusion scan. The scan area included the tumour centre level, and adopted film scanning technology (1 r/0.5 s), with a thickness of 5 mm/4 i, a reconstruction slice thickness 10 mm/2 I; the scan was taken at 80 kV and 200 mA. Rapid intravenous bolus injection of contrast medium was done using a high-pressure syringe through the right elbow, with a flow rate of 3.5 ml/s, total dose of 50 ml, delay time of 5 s and a total scan time of 50 s.

Image processing and analysis

The Adw 4.0 workstation was used for image analysis. Perfusion 2 software was applied to perfusion imaging, including the following steps: (1) select the perfusion image; (2) image calibration by adjusting the lateral deviation of the image; (3) select the inflow arteries (anterior cerebral artery, multiple choices) and the outflow vein (superior sagittal sinus, multiple choices), then the perfusion images were calculated and displayed; (4) show PS perfusion images and set the regions of interest (ROI) in the lesion centre, edge and surrounding tissue. The size of the ROI should be appropriate for reflecting the strengthened characteristics of the region. We set three ROIs in each locale, then calculated the average PS value.

VEGF immunohistochemical staining

The SP method was used with an SP kit and DAB chromogenic kit. Three regions were observed (within the tumour edge and the surrounding tissue) for each case and three high power fields (200×) were randomly selected to give a continuous count of 100 cells for each region. We defined those areas with more than 20% positive cells as high expression areas using granular brown staining as the positive standard.

Statistical analysis

The SPSS statistical package was used for t-tests and χ^{2} test analysis.

Results

Enhanced features of brain metastases and pathological manifestations

Tumours showed ring enhancement in 16 cases, while five cases showed nodular enhancement (Figure 1). The tissue sections showed that tumour cells were arranged around the edge of the tumour biopsy. No capsule was seen, but many blood vessels and the infiltration of inflammatory cells was seen, and many red blood cells were scattered within the stroma in part of the lesion. The tumour interior showed necrosis in 16 cases and had mostly non-structural areas, while five cases showed fewer but more uniformly distributed tumour cells. Tissues around the tumour were loosely organised and glial cells were swelled. We could also see red blood and inflammatory cells.

MSCT perfusion imaging permeability surface (PS) values in brain metastasis tissues

MSCT perfusion imaging showing the permeability surface is shown in Figure 2. The PS values were high in the ring enhanced tumour margins and nodule enhanced tumour interiors, showing significantly as high-performance and transparent red. The PS values of the tumour margin and ring enhanced tumour interior were lower, showing as blue-violet and low-pass performance. The average PS values of the tumour interior, edge and the surrounding tissue are shown Table 1. The PS value distribution in these cases is shown in Table 2. In ring enhanced tumours, the PS value of the edge tissue was higher than the internal and surrounding tissues, while the PS value of the edge tissue was higher than the internal and surrounding tissue in nodular enhanced tumours. According to the t-test, PS values between the edge tissue and the internal as well as surrounding tissue were significantly different ($t = 10.473$ and $t = 12.326$, $P < 0.01$), while the tumour internal and surrounding tissues showed

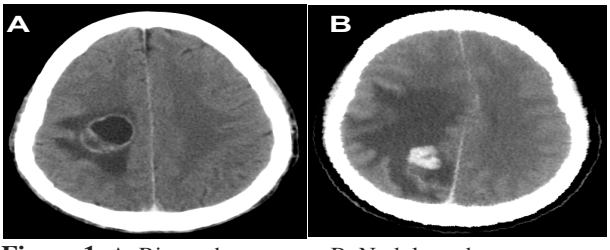

Figure 1. A. Ring enhancement. B. Nodular enhancement

Table 1. The Average Permeability Surface (PS) Values (ml/min/100mg) **in Tumour Tissues**

Enhancement type	Tumour internal tissues	Tumour edge tissues	Surrounding tissues
Ring enhanced	0.742	31.194	5.3127
Nodule enhanced	24.845	29.776	2.7975

Table 2. The Expression of VEGF in Different Areas of Tumours And Permeability Surface (PS) Value Distribution (number of cases)

Checked area	VEGF high expression	VEGF low expression	PS value high	PS value low
Tumour interior	5	16	5	16
Tumour edge	18	3	20	1
Surrounding tissues	0	21	0	21

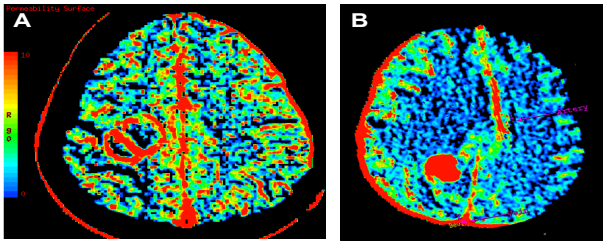

Figure 2. A. CT perfusion imaging showed PS values of Figure 1 and 3 showing higher PS values at the edge rather than the centre of the lesion. B. CT perfusion imaging showed the PS value between the edge and the centre of the lesion have no significant difference

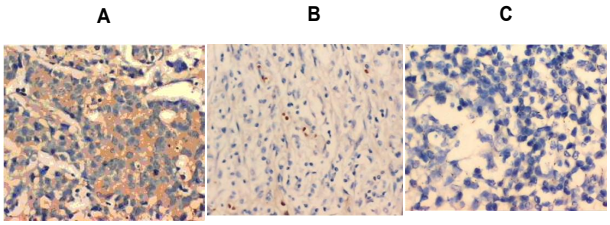

Figure 3. A. VEGF staining of the edge of brain metastases showing more stained cells and obviously stained cytoplasm (200×). B. VEGF staining in the centre brain of metastases showing fewer stained cells and lightly stained cytoplasm (200×). C. No apparent VEGF positive cells were found in the tissues surrounding brain metastases

no significant difference (t=1.347, P> 0.05).

VEGF expression in tumour

All tumours had different levels of VEGF expression. The results on the distribution of VEGF expression in the tumour interior, edge and the surrounding tissue in these cases are shown in Table 2. Marginal zone tumour VEGF expression was significantly higher, while VEGF in central brain metastases showed lower expression (Figure 3).

Correlation between VEGF expression and tumour tissue permeability surface (PS) value distribution

According the $\chi^{-square}$ test, $\chi^2 = 6.67$, $P < 0.01$, so VEGF expression and PS values were significantly correlated.

Discussion

Petchell (2003) reported that with the improvement of medical imaging technology, more and smaller metastases are detected early. As a result, the clinical incidence of brain metastases continues to rise, accounting for about 40% of intracranial tumours. To improve quality of life, we need more diagnostic technologies to diagnose brain metastases at an early stage and to perform treatment monitoring. Modern molecular biology has deepened our understanding of diseases, especially cancer, on the protein and gene levels, and has resulted in the development of molecular pathology, tumour immunology and other emerging interdisciplinary fields. In theory, molecular pathological changes caused by the expression of genes and cytokines can be directly or indirectly imaged. Therefore, we performed early-stage cancer detection, positioning, and monitoring by studying the imaging findings of brain metastases and their molecular mechanisms.

Folkman (1971), as early as 1971, first stated his hypothesis that could explain the significance of tumour angiogenesis in tumour development, transfer and diffusion, and suggested that angiogenesis inhibitors may become a new, valuable cancer treatment. Folkman's hypothesis considered that tumour angiogenesis plays an important role in cancer biological behaviour. When a tumour grows to ~1-2mm, it must induce new blood vessel growth to supply nutrition. Solid tumour growth depends on angiogenesis and the process is regulated by genes, cytokines and other complex factors, especially VEGF. VEGF, a glycosylated and secreted polypeptide, plays an important role in brain tumour formation. It has a wide range of expression from the embryonic development stage, although it is tightly regulated with a low level of expression under normal physiological conditions. When tumour growth induces strong angiogenesis, VEGF is highly expressed to promote endothelial cell division, proliferation and new blood vessel growth toward the tumour. At the same time, it can significantly increase tumour vascular permeability. Currently, there are many ways of treating cancer that use vascular inhibitors to control tumour angiogenesis, tumour growth and metastasis (O'Reilly et al., 1997; Dhanabal et al., 1999; Dixelius et al., 2000). In the central nervous system, VEGF expression is closely related to the blood-brain barrier damage (Christiana, 2003; Napoleone et al., 2003). Studies have shown that VEGF expression and microvessel density are well correlated (Tynninen et al., 1999). VEGF plays an important role in angiogenesis and blood-brain barrier for neurological changes. Its effect on the blood-brain barrier may be to increase vascular permeability by affecting the close association between the brain microvascular epithelial cells.

The CT perfusion imaging dynamic scan selected layers after intravenous bolus injection with a contrast agent to obtain time-density curves (TDC) for each pixel

in a layer. The curve used a different mathematical model law (central volume principle) where BF=BV/MTT (blood flow, BF; blood volume, BV; mean transit time, MTT). We can obtain the time-activity curve of the radioactive tracers injected through the intravenous bolus that reaches an organ through the left ventricle; dynamic scanning can be used to determine when the tracer arrives at an organ. Miles (Cenic & Nabavi, 2000) have suggested that radiographic contrast agents injected intravenously have the same pharmacokinetics as radioactive tracers, so radionuclide tracer principles can be used for dynamic CT studies. Some studies have shown that tumour PS values depend on whether the tumour is benign or malignant. Also it has maximum value among the technical parameters of CT perfusion. The PS value parameter is mainly used in the evaluation of tumours, as it refers to the rate of contrast agent leakage from the intravascular space into the tissue space in one direction; the units are ml/min/100 mg (Eastwood et al., 2001; Roberts et al., 2002).

In the 21 patients with brain metastases investigated in this study, five cases showed nodular enhancement and 16 cases showed ring enhancement. They were summarised as cystic nodules (Wintermark et al., 2001). In 18 cases, the tumour edge showed high VEGF expression, with high cell density at the tumour biopsy edge and more vascular structures. When the ultrastructure was observed, we could see the latch emerged small cracks, a discontinuous basement membrane, loose fibre structure and the formation of a fenestrated structure which was similar to the blood vessels of the sources tissue. In the ring enhanced cases, we could observe fewer tumours with necrotic interiors, with more widely distributed tumour cells and lower expression of VEGF. The CT perfusion images showed that the PS value was high at the tumour edge of 20 metastatic tumours. The vascular permeability of the tumour edge was significantly higher than the interior of the ring enhanced tumours. High vascular permeability distribution and high expression of VEGF had a significant spatial correlation, and thus to a certain extent, we can speculate on the expression of VEGF using CT perfusion images. In two cases included in this study, the PS values of tumour edge were high while VEGF showed a lower expression, which may have been related to the VEGF immunohistochemical staining technique.

In summary, there was a significant correlation between tumour VEGF expression in brain metastases and the PS value of CT perfusion images. This is based on the expression of VEGF which promotes angiogenesis. In the regions where VEGF was expressed at a higher level, angiogenesis was more apparent and the PS value was greater. The analysis of CT perfusion image for brain metastases can help forecast the expression level of VEGF and monitor the treatment effect of brain metastases.

References

Cenic A, Nabavi DG (2000). A CT method to measure hemodynamics in brain tumors, validation and application of cerebral blood flow maps. *AJNR Am J Neuroradiol*, **21**, 462-70.

Christiana Ruhrberg (2003). Growing and shapping the vascular tree, multi-ple roles for VEGF. *Bio Essays*, **25**, 1052-60.

Dixelius J, Laesson H, Sasaki T, et al (2000). Endostasin induced tyrosinekinase signaling through the Sh adaptor protein regulates endothelial cell apoptosis. *Blood*, **95**, 3403-11.

Dhanabal M, Ramchandran R, Waterman MJ, et al (1999). Endostasin induces endothelial cell apoptosis. *J Biol Chem*, **274**, 117-21.

Eastwood JD, Provenzale JM, Hurwitz LM, et al (2001). Practial injection-rate CT perfusion in a case of stroke. *Neuroradiology*, **43**, 223.

Folkman J (1971). Tumor angiogenesis, therapeutic implications. *N Eng J Med*, **285**, 1182-6.

Hanahan D, Folkman J (1996). Patterns and emerging mechanisms of the angiogenic switch during tumorsigenesis. *Cell*, **86**, 353-64.

Hermans R, Meijerink M, Van den Bogaert W, et al (2003). Tumor perfusion rate determined noninvasively by dynamic computed tomography predicts outcome in head-and-neck cancer after radiotherapy. *Int J Radiat Oncol Biol Phys*, **57**, 1351-6.

Hoeffner EG, Case I, Jain R (2004). Cetebral perfusion CT, technique and clinical application. *Radiology*, **23**, 632-44.

Jeffrey MR, Nina M, William F, et al (1998). Patterns of brain angiogenesis after vascular endothelial growth factor administration in vitro and in vivo. *Neurobiology*, **95**, 7086-91.

Miles KA, Hayball M, Dixon AK (1991). Colour perfusion imaging, a new application of computed tomography. *Lancet*, **337**, 643-5.

Napoleone F, Hans PG, Jennifer L (2003). The biology of VEGF and its receptors. *Nat Med*, **9**, 669-76.

O'Reilly MS, Boehm T, Shing Y, et al (1997). Endostasin, An endogenous inhibitor of angiogensis and tumor growth. *Cell*, **88**, 277.

Petchell RA (2003). The management of brain metastases. *Cancer Treat Rev*, **29**, 533-40.

Principi M, Italiani M, Guiducci A, et al (2003). Perfusion MRI in the evaluation of the relationship between tumour growth, necrosis and angiogenesis in glioblastotnas and grade 1 meningiomas. *Neuroradiolagy*, **45**, 205.

Purdie TG, Henderson E, Lee TY (2001). Functional CT imaging of angiogenesis in rabbit VX2 soft-tissue tumor. *Phys Med Biol*, **46**, 3161-75.

Roberts HC, Roberts TP, Lee TY, et al (2002). Dynamic, contrast-enhanced CT of human brain tumors, quantitative assessment of blood volume, blood flow, and microvascular ermeability, preport of two cases. *AJNR Am J Neuroradiol*, **23**, 746-7.

Roberts HC, RobertsTP, Smith WS, et al (2001). Multisection dynamic CTperfusion for acute cerebral ischemia, the "toggling-table" technique. *AJNR Am J Neuroradiol*, **22**, 1077.

Shin JH, Lee HK, Kwntn BD, et al (2002). Using relative cerebral blood flow and volume to evaluate the histopathologic grade of cerebral gliomas, preliminary results. *AJNR Am J Neuroradiol*, **179**, 783-9.

Tynninen O, Aronen HJ, Ruhala M, et al (1999). MRI enhancement and microvascular density in gliomas. Correlation with tumor cell proliferation. *Invest Radiol*, **34**, 427-34.

Wen W, William LD, Ronald TB (2001). VEGF increases BMEC monolayer permeability by affecting occludin expression and tight junction assembly. *Am J Physiol Heart Circ Physiol*, **280**, 434-40.

Wintermark M, Thiran JP, Maeder P, Schnyder P, Meuli R (2001). Simuitaneous measurement of regional cerebral blood flow by Perfusion CT and stable xenon CT, A validation study. *AJNR Am J Neuroradiol*, 22, 905-14.